Simulation Studies on Air Fluorescence and Cerenkov Lights from UHE Air Showers for EUSO Experiment

Yuya Fukushima,[1] Yoshimitsu Wada,[1] Naoya Inoue,[1] Hristofor P. Vankov,[2] and EUSO collaboration
(1) Department of Physics, Saitama University, Saitama-city, Saitama 338-8570, Japan
(2) Institute for Nuclear Research and Nuclear Energy, Sofia, Bulgaria

Abstract

EUSO experiment plans to observe Ultra High Energy(UHE) air showers with an effective area of 120000km^2 from a satellite's orbit, to solve the astrophysical problems on UHE cosmic ray origin, acceleration and related topics on the highest energy particle interactions. Simulation studies have been carried out, to determine the optimized device performance and to establish the analysis procedure for the determination of primary energy, arrival direction and position of shower maximum. In this paper, the performance of EUSO detector is discussed from the points of resolutions of such air shower parameters.

1. Introduction

In a recent report, 11 air shower events which attains to 10^{20}eV have been observed by AGASA experiment[1]. Their source and acceleration mechanism are still mystery and hot subjects in the field of high energy particle astrophysics. The cosmic ray with an energy exceeding $10^{19.6}$eV is expected to interact with 2.7–K background radiation and to lose its primary energy. The hypothesis (GZK cutoff[2]) predicts a sharp cutoff in primary cosmic ray spectrum. However, the resultant cutoff is not clearly confirmed experimentally. EUSO experiment, which will be installed at International Space Station, is one of planned observations for Super–GZK energy events with a large effective area of 120000km^2.

Japanese EUSO group has taken part of the development of photo–sensitive device. This simulation has been developed as a probe for estimating the detector ability on shower observation. In this simulation, fluorescence and Cerenkov photons from electrons in showers have been estimated by taking into account atmospheric attenuation, response of optical system and characteristics of photo–sensitive device.

2. Simulation Procedure

Current simulation is based on the Gaisser-Hillas formula[3] as an assumed shower profile initiated by primary proton. Although this is an average shower profile, sampling the first interacting point introduce one of the main sources of longitudinal shower fluctuations. The depth of shower maximum(X_{max}) as a function of energy, which assumed in the function was calculated by AIRES simulation code(Ver.2.6.0)[4].

pp. 603–606

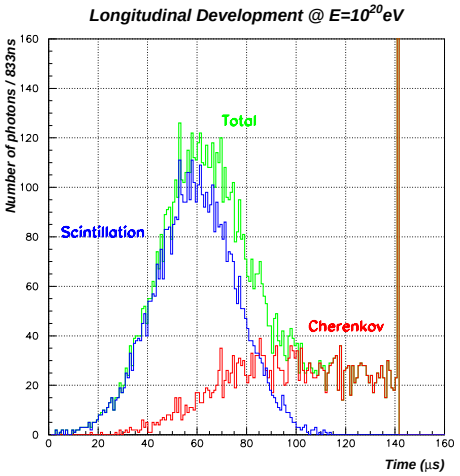

Fig. 1. An example of arrival time distributions of ASPs and ACPs in GTU unit for a shower of 10^{20}eV and 60^o.

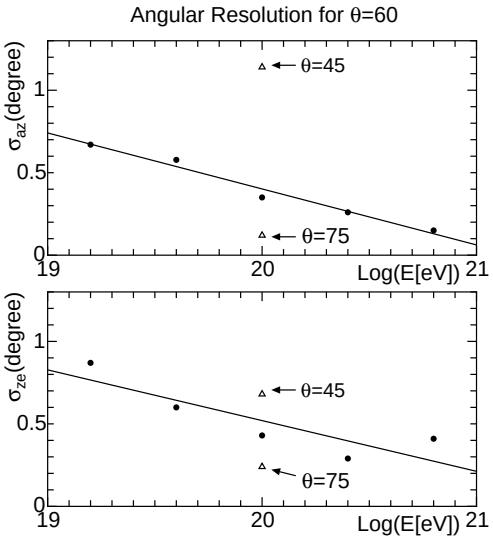

Fig. 2. Standard deviations(σ_{ze} and σ_{az} for θ and ϕ, respectively) of angular differences between a real direction and output one.

Along the shower development, the number of electrons was estimated with a step of 10gcm^{-2} and emitted Atmospheric–Scintillation–Photon(ASP)s with 6 typical wavelengths(314,336,357,381,392,402nm in a region of 300nm to 450nm[5]) were calculated. The altitude dependence of photon yield was also approximated by the following,

$$N_{fluo}(h) = -7.80 \times 10^{-9} h^2 + 1.35 \times 10^{-4} h + 3.73 \tag{1}$$

where, N_{fluo} is total ASPs yield at a vertical height h in meter. Atmospheric–Cerenkov–Photon(ACP)s were also generated along a shower axis in every 10gcm^{-2} step and their emission angles were treated as parallel to the axis. ACPs in the direction of EUSO site were calculated as scattered ones by Rayliegh scattering using the following functions.

$$\frac{dN}{dx} = -\rho \frac{N_0}{X_{R(400)}} \left(\frac{400[nm]}{\lambda} \right)^4, \qquad \frac{d^2N}{dx d\Omega} = \frac{dN}{dx} \frac{3}{16\pi} (1 + \cos^2\theta) \tag{2}$$

In addition, a reflected component of ACPs at the earth surface(Cerenkov Mark:CM) was estimated as simple assumptions of a uniform reflection angular distribution and a reflection coefficient of 20%. Arrival ASPs and ACPs at the optical lens of EUSO were finally calculated after taking into accounts of absorptions by Rayliegh scattering in the atmosphere as a function of wavelength and by Ozone component as 10% absorption for an overall wavelength. In this calculation, curvatures of earth surface and atmospheric layer were incorporated and U.S. standard atmospheric model, 1976 was assumed.

ASPs and ACPs impinging on the optical system were converted to photoelections and then each photoelectron were recorded with the information of parent photon's wavelength, arrival direction, arrival time and position in a coordinate axis of

the focal surface. Here, a ray–trace sub-code, which examined an effect of absorption, aberration and scattering in the optical system was used. 5x5 channel multi-anode PMT(R8900–03–M25: HAMAMATSU) with a pixel size of 5mmX5mm was assumed as a photo–sensitive device to analyze produced photoelectrons at the focal surface.

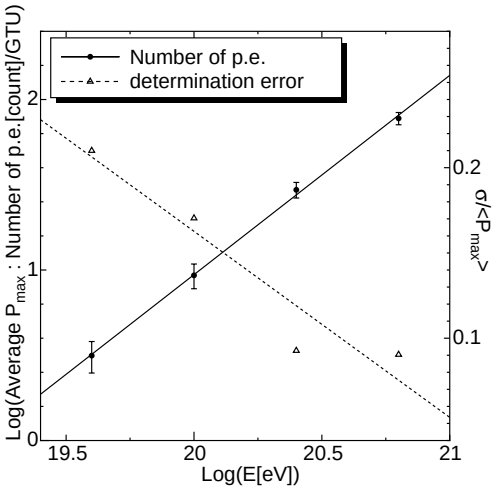

Fig. 3. $< P_{max} >$ and standard deviation of P_{max} normalized by $< P_{max} >$ as a function of energy.

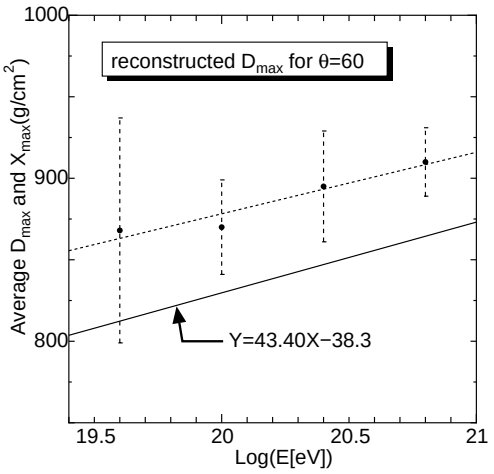

Fig. 4. $< D_{max} >$ with standard deviation as a function of energy. A relation between $< X_{max} >$ and energy assumed in a shower generation code is drawn by a solid line.

3. Results

Primary protons with energies in a region of $10^{19.2}$–$10^{20.8}$eV, a zenith angle(θ) = 60^o and a uniform distribution of azimuth angle(ϕ) were mainly assumed for generations of ASPs and ACPs. Their core locations were fixed at the center of field of view. The reconstruction process was applied for the number of simulated photoelectrons in each pixel and arrival time in Gate–Time–Unit(1GTU=833ns). Diffusive emissions of atmospheric O_2 and N_2 which raise to 0.5 photoelectrons/pixel·GTU, were not included in the process of reconstruction as the background photons.

An example of arrival time distributions of ASPs, ACPs in GTU is shown for a shower with an energy of 10^{20}eV and θ of 60^o in figure 1. Though arrival time distribution of ASPs follows nearby the shower longitudinal development, a forward emitting ACP component becomes measurable in the latter stage of development and finally a remarkable signal of CM emerges in the right side of the distribution.

Figure 2 shows standard deviations(σ_{ze} and σ_{az} for θ and ϕ, respectively) of angular differences between a real direction and output one for 100 simulated events for each energy. Also in the same figure, ones for $\theta = 45^o$ and 75^o are drawn at 10^{20}eV. The determination errors of arrival directions becomes smaller with an increase of primary energy and θ, i.e. both σs become less than 0.5^o for regions of $\geq 10^{20}$eV and $\theta \geq 60^o$.

Individual arrival time distribution of photoelectrons was fitted by the least square method with a following function,

$$N_{p.e.} = a_2 \times \exp\left[-2a_3\left(\frac{t-a_1}{t+2a_1}\right)^2\right] \quad (3)$$

where, $N_{p.e.}$ is the number of photoelectrons at a time of t in GTU. Average photoelectron numbers at maximum in a GTU($< P_{max} >$) and atmospheric depth at $< P_{max} >$ in gcm^{-2} ($< D_{max} >$) were determined from the reconstructed shower axis and the relative time difference between $< P_{max} >$ and CM. In figure 3, $< P_{max} >$ and standard deviation of P_{max} normalized by $< P_{max} >$ are shown for 4 different energies. A relation between $< P_{max} >$ and energy is well expressed by a power law with an index of about 1.17. $< P_{max} >$ in a GTU and normalized standard deviation are approximately 10 and 16% at an energy of 10^{20}eV, respectively.

$< D_{max} >$ with a standard deviation indicated by a bar is shown in figure 4 as a function of energy. In the same figure, a relation between average $X_{max}(< X_{max} >)$ and energy which was assumed in a shower generation code, is also drawn by a solid line. $< D_{max} >$ is systematically shifted to be larger than $< X_{max} >$ by ~ 50gcm^{-2}. As mentioned in relation to figure 1, $< D_{max} >$ is affected by not only ASPs but ACPs, so the discrepancy is possible to be caused essentially by a contribution of ACP component. Therefore, a careful examination of ACP contribution to shower development in a process of reconstruction will be required to determine an energy and X_{max}.

The number of photoelectrons from CM was about 20 even at an energy of 10^{19}eV and increased as energy with a power law index of 1.02 from this simulation. A wavelength distribution of CM photons is shifted to longer wavelength region compared to one of ACPs because a longer wavelength component of ACPs is accumulated along a shower development and becomes a source of CM photons. The detection of CM photons will be helpful for determinations of shower axis and shower development.

Acknowledgements.

We thanks Dr.Y.Kawasaki and N.Sakaki in RIKEN Institute, Wako, Japan for a helpful discussion on ray-trace code and photosensitive device. Present study was supported by Grants-in-Aid for Scientific Research, programmed by JSPS.

4. References

1. Takeda M. et al. 2002, astro-ph/0209422(Astroparticle Physics in press)
2. Greisen K. 1966, Phys. Rev. Lett., 16, 748, Zatsepin G.T. and Kuz'min V.A. 1966, JETP Lett., 4, 78
3. Gaisser T.K. and Hillas A.M. 1977, Proc.15th ICRC(Plovdiv), 8, 353
4. Sciutto S.J. 1999, astro-ph/9911331
5. Nagano M. et al., 2003, Astroparticle Physics, 19, 447(astro-ph/0303193)